Trans. JWRI, Vol. 22 (1993), No.1

Development of Computer Aided Process Planning System for Plate Bending by Line-Heating (Report III)†

- Relation between Heating Condition and Deformation -

Yukio UEDA*, Hidekazu MURAKAWA**, Ahmed Mohamed RASHWAN***, Isao NEKI****, Ryoichi KAMICHIKA****, Morinobu ISHIYAMA**** and Jun-ichiro OGAWA****

Abstract

An effective plate bending process by line-heating can be achieved when the heating conditions are properly selected to produce desirable bending or inplane deformations. To make such decisions on the heating condition, the relation between heating conditions and deformations must be clarified. For this purpose, the authors studied the similarity rule holds for the line-heating process and derived two parameters governing the deformations. Also, new 3-dimensional F.E.M. codes are developed as versatile tools to replace costly experiments. Their validity is examined through a comparison with an experiment and it is applied to study the general relations between the parameters and the deformations of plates.

KEY WORDS: (Line-Heating) (Inherent Deformation) (Similarity) (Heating Condition) (Angular Distortion) (Shrinkage) (Finite Element Method) (Experiment)

1. Introduction

In the plate bending by the line-heating method, the plastic deformations are created as a result of the heating and the cooling processes. The plate is bent under the effect of these plastic deformations. The behavior of the plate during the heating and cooling cycle is of complex nature and the shape obtained after the heating is difficult to predict a priori. In order to automate the process, the following informations such as, (a) the position and the direction of heating lines, (b) the proper heating and cooling condition to get the necessary deformation are necessary. To determine the position and the direction of heating lines, the relation between the final form of the plate and the inherent strain to be given has been studied using the Finite Element Method[1-2]. The correlation between the inherent strain and the final form has been clarified and a fundamental idea to decide the position and the direction of heating lines has been proposed. The validity of the proposed idea has been examined using mathematical and real curved shapes.

Once these decisions are made, it is necessary to chose the proper heating conditions for getting the required inherent strain or deformation at each heating line. To determine the heating condition, two different analyses are required, namely heat condition and thermal-elastic-plastic deformation analyses. The most significant factors affecting both fields are the heat input rate, the moving speed of the heat source and the thickness of the plate. There are other secondary factors which may affect the deformation of the plate, such as the length and the width of the heating line, the heat input distribution, the initial curvature and the residual stress of the plate, etc. All of these factors have some influence on the inherent deformations produced by the line-heating. Although there are a few reports dealing with the experimental and the theoretical studies on these factors, the information available is rather limited[3-12].

To get the comprehensive understandings on the relation between the heating conditions and the resulting inherent deformation, large number of experimental and/or numerical analyses are required to cover the possible range of these factors affecting the process. In such a situation, similarity rule can be introduced to reduce the number of cases to be studied. Thus, two parameters governing the similarity rule are derived.

† Received on August 2, 1993
* Professor
** Associate Professor
*** Graduate Student
**** Ishikawajima-Harima Heavy Industries Co., Ltd.

Transactions of JWRI is published by Welding Research Institute, Osaka University, Ibaraki, Osaka 567, Japan

In general, numerical simulations become superior to physical experiments due to the great advancement in computer technology today. The Finite Element Methods is considered to be one of the most effective tool to replace the costly experimental work. Therefore, 3-D F.E.M. codes for both the heat conduction and the thermal-elastic-plastic deformation analyses are developed. The validity of these codes are examined through a comparison with the experiment done using the induction heating. These F.E.M. codes are applied to study the relation between the line-heating conditions and the inherent deformations. The computed results are classified based on the proposed parameters.

2. Method of Analysis

The mechanism of the plate bending using line-heating method is highly complicated to be analyzed with simple analytical methods. The difficulty involved in the problem comes from the material and the geometrical nonlinearities as well as the variation of the temperature in spatial and time domains. The study of thermal-elastic-plastic behavior of the line-heating process has received an attention from about 3 decades ago. The first attempt to use an analytical approach to simulate the line-heating process was done by Suhara[4] and Iwasaki et al.[7] They modeled the problem using the beam theory and the solution was obtained analytically. Due to these restrictions, their model can deal with only ideal situations. Iwamura and Rybicki [8] also analyzed the process using a beam model which is normal to the heating line and they employed the finite difference approach in solving the problem. Moshaiov and Vorus[10] developed a boundary element method based on the thermal-elastic-plastic plate bending theory. The limitation of their method is that only small deflection is considered in the theory. Also, Moshaiov and Shin[11] had modified the strip model and extended it to uncoupled thermal-elastic-plastic strip. In this modification, they imposed artificial temperature and material properties to avoid coupling between the bending and the inplane problem. These assumptions may be improper to analyze the real behavior of the plate during the heating and the cooling processes.

The Finite Element Method[13] is considered to be the most effective tool for various engineering analyses. With the fast and great advance in the computer technology, the limitations on numerical simulations have been removed. To analyze the behavior of the plate under line-heating process, 3-D thermal-elastic-plastic Finite Element Method in which large deformation is considered has been developed. Solid elements with selective reduced integration is employed to avoid the transverse shear locking[14),15)]. In addition, to account for the temperature variation through the thickness, 3-D Finite Element Method for the heat conduction problem has been also developed. The validity of the developed FEM codes are examined through an experiment using the induction heating.

3. Validation of F.E.M. Codes

3.1. Features of experiment

In the plate bending process, the gas torch is commonly employed as a heat source. An alternative heating method which has been studied is the laser heating[16]. When gas heating is used, it is difficult to control the amount of heat input power during heating. On the other hand, the laser is superior in the controllability and its applicability has been studied. However, it requires a special instruments which are complex and very expensive. Further investigation is necessary to introduce the laser into the plate bending in ship yards.

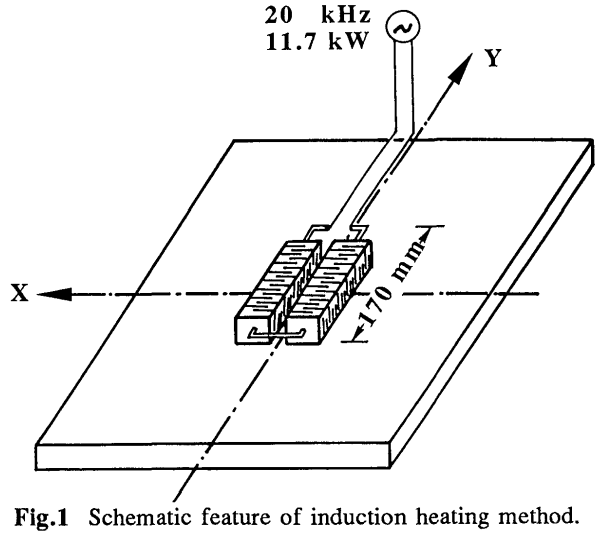

Fig.1 Schematic feature of induction heating method.

Another alternative heat source with high controllability is the induction heating. To verify the F.E.M. codes, the experiment of line heating using induction coil is done. The schematic representation of the induction heating method is shown in **Fig.1** . The length of the induction coil is 170 mm and its effective heating width is roughly 20 mm. The effective heat input power is 11.7 kW and the frequency is 20 kHz. The efficiency of the heating is about 0.8. The effective depth of the heating zone is observed to extend 2 mm below the heating surface. The mechanical and the thermal properties of the material used in the experiments are shown in **Figs.2** and **3**.

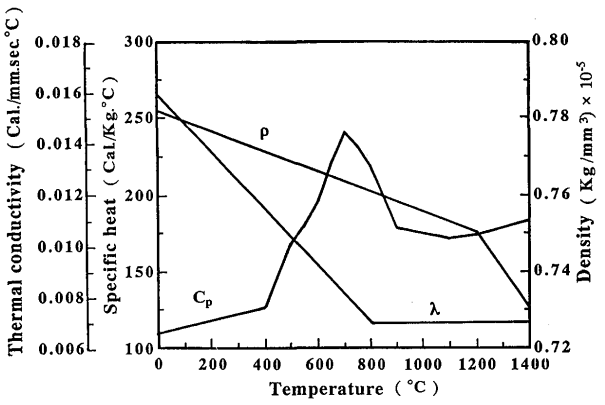

Fig.2 Temperature dependent thermal properties of steel.

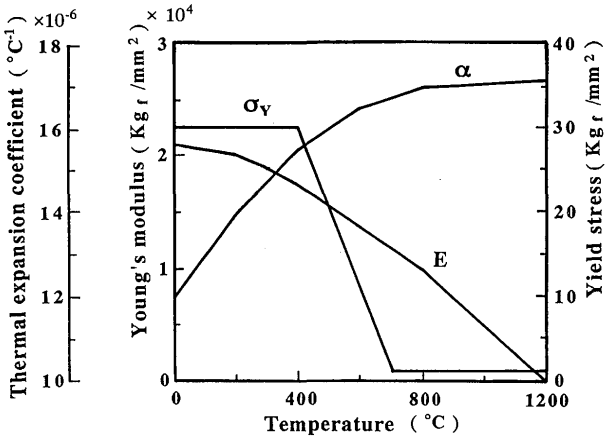

Fig.3 Mechanical and physical properties as functions of temperature.

The dimensions of the model used in experiment are 500×500×16 mm as shown in **Fig.4** . The distribution of the heat input is assumed to be constant along the length of the coil. In the width direction, it is assumed to distribute as shown in **Fig.5** which describes the distribution of the heat input per unit volume of the heated layer. The duration of the heat input was 40 seconds for the temperature measurements. The heat source was kept fixed at the center of the plate and the longitudinal axis of the coil was set parallel to *y*-axis. The thermocouples were placed at different positions and only three positions A, B and C are selected for comparison. The coordinate of these points are (0.0,0.0,1.1), (10.0,0.0,1.3) and (0.0,15.0,16.0), respectively, as shown in Fig.2.

3.2 Temperature field

In the computation, the heat input is given to the elements within 2 mm from the surface of the plate. Due to the symmetry, only one quarter of the model is analyzed. The mesh division used in the computation is

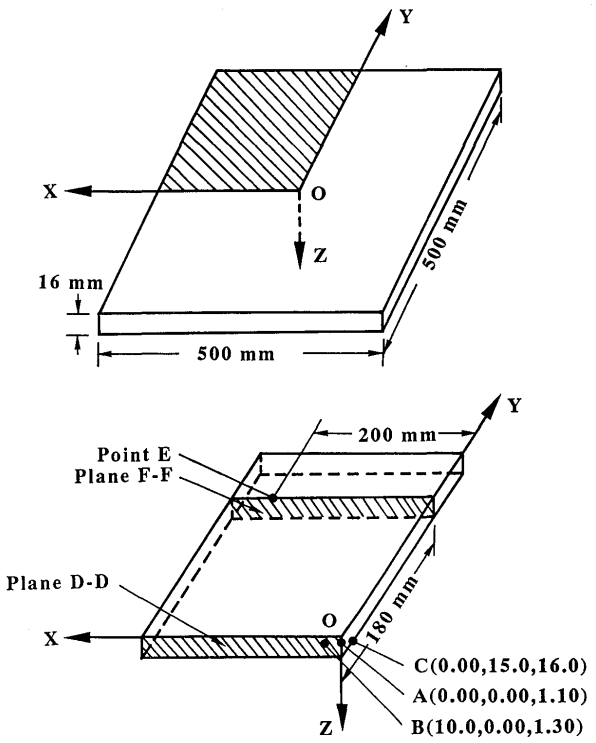

Fig.4 Model for experiment and location of thermo-couples.

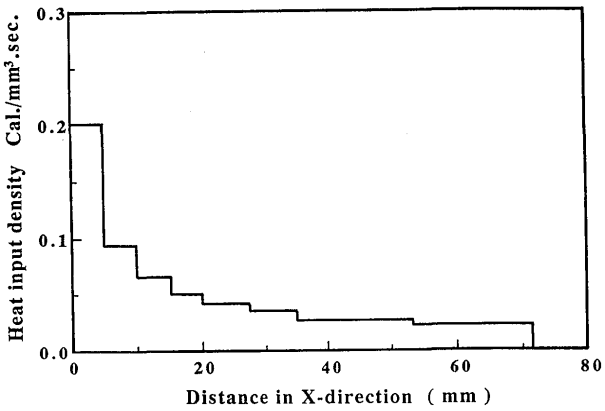

Fig. 5 Heat input distribution in width direction.

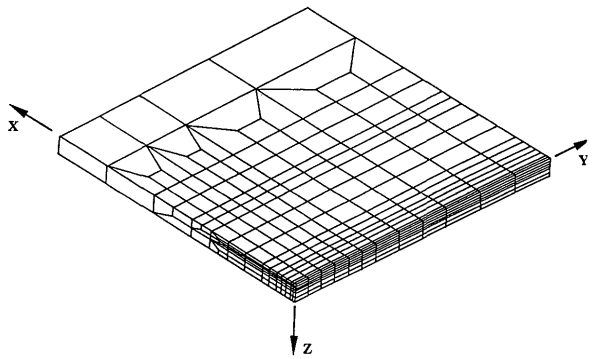

Fig.6 Mesh division.

shown in **Fig.6**. The finer divisions are used in the thickness and the length directions in the region near the heating line and the course divisions for the region away from the coil. The computed and the measured temperature histories at the points A, B and C are shown in **Fig.7**. The computed temperature at the point A, which is at the center of the coil and 1.1 mm below the heated surface, is slightly smaller than the measured one. At the point B, which locates 10 mm off the centerline of the coil and 1.3 mm below the surface, good agreement is observed. While, the computed temperature is about 15 % higher than the measured one at the point C on the back surface. This means that the gradient of the computed temperature through the thickness is relatively smaller than that of the experiment. Although, there is a small discrepancy, the computed temperatures show generally good agreements with the experimental ones. This proves the validity of the developed F.E.M. code for the heat conduction problem.

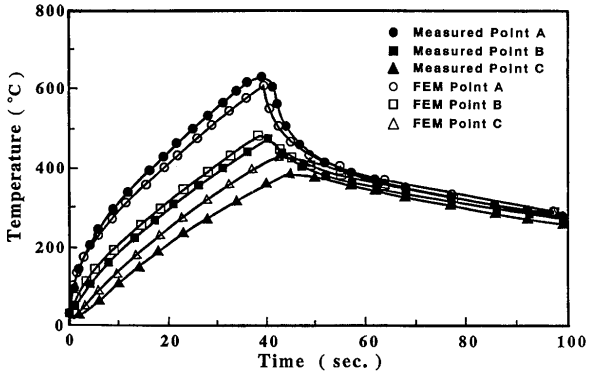

Fig.7 Comparison between computed temperature history at points A, B and C.

3.3 Deformation field

The same model as in the temperature measurements was used for the measurements of deflection except that the duration of heating was chosen to be 60 seconds. The stress-strain relationship is assumed to be elastic-perfect-plastic. The deflections of the top and the bottom surfaces of the plate were measured at different points along two planes, D-D and F-F as shown in Fig.2. The plane D-D is the transverse cross-section at the center of the plate and the plane F-F is that near from the edge as shown in Fig.2. The same mesh division used for computing the temperature is used for the deflection.

The computed and the measured values of deflection at the two planes D-D and F-F on the top and the bottom surfaces of the plate are shown in **Figs.8** and **9**, respectively. The value of the deflection is defined relative to that of the point E which is chosen as a reference. From these figures, it can be noticed that the measured and the computed deflections have the same trend. When the computed deflection in Fig.8 is closely examined, it is noticed that local swelling of the plate at the heated area precisely agree with the experiment. The increase of the thickness due to the swelling is about 0.2 mm and it almost coincides with the experiment. This kind of local swelling is caused by large transverse shrinkage due to the plastic deformation and the incompressibility of the plastic deformation. The expansion in the thickness occurs to maintain the incompressibility under the transverse shrinkage.

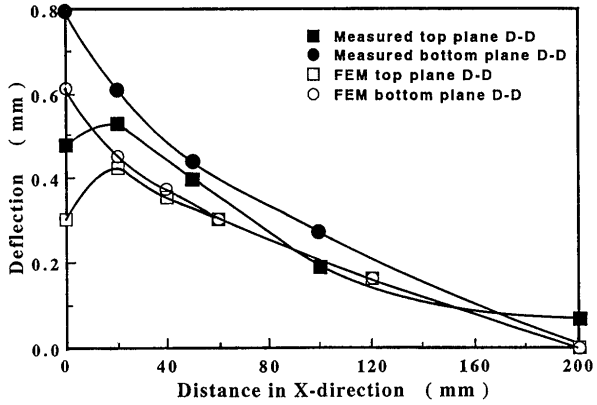

Fig.8 Computed and measured deflection on top and bottom at plane D-D.

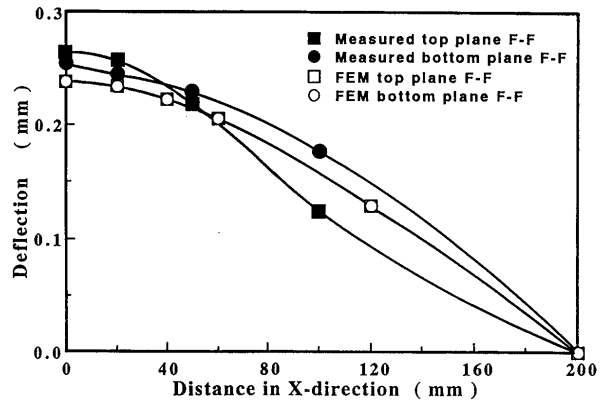

Fig. 9 Computed and measured deflection on top and bottom at plane F-F.

As seen from the computed results in Fig.9, there should be no difference in deflection between the top and the bottom surfaces of the plate away from the heating line. Hence, the difference observed in the measured deflections are the error in the measurements. Noting that the magnitude of the error in the measurement is about 0.1 mm, the accuracy of the computed deflection

is satisfactory compared with the measurements and this proves the validity of the developed F.E.M. code for the deformation analysis.

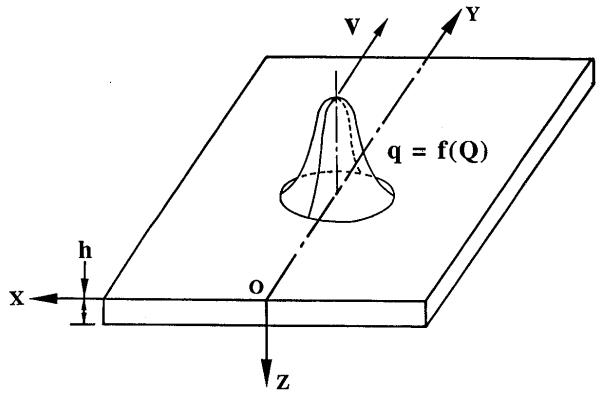

Fig.10 Schematic representation of variables affecting line-heating.

4. Parameters Governing Deformations Produced by Line-Heating

4.1 Governing parameters

The thermal and the mechanical phenomena are governed by various factors. When the material of the plate is the same, the primary factors are heat input rate Q, thickness of the plate h and the moving speed of the heat source v as shown in **Fig.10**. As the secondary factors, the heat input distribution, method of cooling, material properties of the plate, such as the yield stress, dimensions of the plate, initial curvature and the stress may influence the deformation of the plate. The effect of the three primary factors are examined first and then the effect of the heat input distribution is studied in the present work.

To clarify the effect of each factors in a general manner including the physical meaning, the similarity rule which holds in the line-heating process is investigated. Based on this study, two parameters which characterize the process are derived.

The problem of line-heating consists of two sub-problems, namely thermal conduction problem and the thermal-elastic-plastic deformation problem. When the effect of the mechanical field on the thermal field can be ignored, the coupling between the above two problems are removed and they are solved separately. Thus, the similarity rules are also studied individually. For simplicity, the material properties related to the temperature field, such as thermal conductivity λ, specific heat c_p, density ρ and thermal transfer coefficient γ are assumed to be independent on the temperature. Only the Young's modulus E and the yield stress σ_Y are assumed as functions of the temperature. The geometrical nonlinearity is considered in the deformation analysis of the plate.

The details of the discussion on the similarity rule are shown in the Appendix. The outline can be summarized as follows. The fundamental assumptions on which the similarity is considered are :

a) The plate and the distribution of the heat input is geometrically similar.
b) The materials of the plates are the same and their thermal and mechanical properties are the same.

Then, the condition for the deformation to be similar is that:

c) The value of the temperature at points with the same dimensionless coordinates in the same dimensionless time must be the same.

Further, the conditions for the same temperature at the corresponding time and the place are:

d) The following two parameters β and ζ must be the same.

$$\beta = Q/(p^2 v h^3)^{0.5} \quad (1)$$

$$\zeta = (vh/k)^{0.5} \quad (2)$$

where,

k : thermal diffusivity defined as,

$$k=\lambda/c_p\rho$$

p : coefficient of heat penetration defined as,

$$p=(\lambda c_p\rho)^{0.5}$$

As it will be discussed in the next section, the physical meaning of the parameter β is the value which is related to the surface temperature. The parameter ζ represents the relative speed of the moving heat source.

4.2 Physical meanings of parameters

The physical meaning of the two parameters proposed in the preceding section is examined by numerical simulations using F.E.M. The numerical model considered is a steel plate of the size 300×300×8 mm. This plate is assumed to be heated along the center line by a moving heat source starting from one end to the other. The heat input rate is Q and the traveling speed is v. As for the material properties, the same Young's modulus E and the yield stress σ_Y as given by Fig.4 are used. The thermal conductivity λ, the specific heat c_p, the density ρ and the thermal transfer coefficient γ are assumed to be independent on the temperature and following values are used,

$\lambda = 0.0160$	cal/mm·sec·°C
$c_p = 0.980$	cal/g·°C
$\rho = 0.00782$	g/mm^3
$\gamma = 0.27 \times 10^{-6}$	cal/sec·mm^2·°C

The heat is applied in the form of heat flux q and its distribution is assumed to be the Gaussian distribution, such that,

$$q(r)=q_{max}e^{-\kappa r^2} \quad (3)$$

where, r is the distance from the center of the heat source and q_{max} is the maximum value of the heat flux at the center. The total heat input rate Q is given by using the concentration coefficient κ as,

$$Q=\pi q_{max}/\kappa \quad (4)$$

In the present model, the value κ is assumed to be 3.1×10^{-3} mm^{-2}.

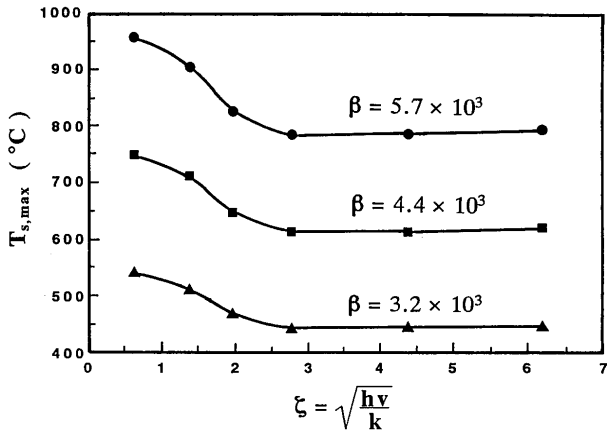

Fig.11 Relation between maximum surface temperature and ζ for constant value of β.

The temperature field in the line-heating process depends primarily on the heat input rate Q, the moving velocity of the heat source v and the plate thickness h. However, similarity holds when certain conditions are satisfied by these three values. Thus, the phenomena are characterized by only two independent parameters β and ζ as shown in Appendix. To clarify the physical meaning of these parameters, serial computations with changing β and ζ are done and the computed results are summarized in **Fig.11**. The maximum surface temperature $T_{s,max}$ for each case is plotted against ζ in the figure. As it is seen from the figure, the surface temperature becomes high as the parameter β becomes larger. The temperature decreases when the moving speed of the heat source becomes large. But it saturates to a constant value in the region $\zeta > 3.0$. The reason for this is that the maximum temperature is influenced by the reflection of the heat flow at the bottom surface when the moving speed is small. If the moving speed is fast enough, the effect of the finiteness of the thickness disappears and the surface temperature becomes constant when β is the same. The region $\zeta < 3.0$ corresponds to the case where the finiteness of the plate is observed in the maximum surface temperature. Thus, the regions in which $\zeta > 3.0$ and $\zeta < 3.0$ are referred to as semi-infinite body response and thick wall response, respectively. When ζ is extremely small, the temperature gradient through the thickness can be neglected. Thus, this region may be classified as the thin wall response.

Further, $T_{s,max}$ normalized by β is plotted against ζ is shown in **Fig.12.** This figure shows that $T_{s,max}/\beta$ is the same when ζ is the same. In other wards, the parameter β is proportional to the maximum surface temperature when ζ is the same. Especially, when $\zeta > 3.0$, $T_{s,max}/\beta$ is almost constant. In such a cases the maximum surface temperature is approximately proportional to β regardless of the value of ζ.

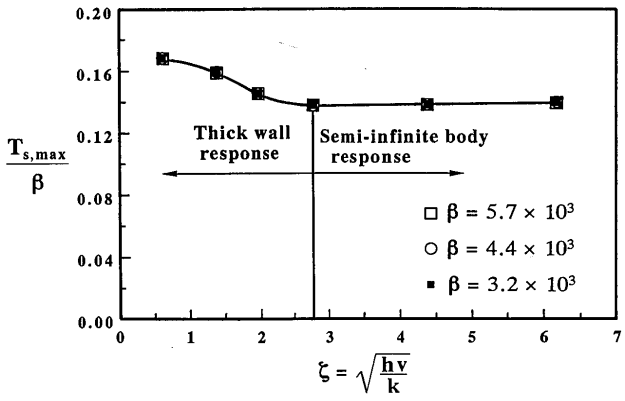

Fig.12 Relation between $T_{s,max}/\beta$ and ζ.

4.3 Verification of similarity rule

To verify the similarity rule, geometrically similar two models shown in **Fig.13** are analyzed by F.E.M. One model is the same model as discussed in the preceding section which has the dimension of 300×300 ×8 mm. Another model is twice as large as the first one with its dimensions 600×600×16 mm. For convenience, these two models are denoted as **M8** and **M16** according to the thickness. To maintain the similarity of the heat input distribution, the concentration coefficient κ are assumed to be 3.1×10^{-3} mm^{-2}, 7.75×10^{-4} mm^{-2}., respectively. The parameter β is assumed to be 4.4×10^3 and two values of ζ corresponding to the thick wall response and the infinite body response, i.e. 1.9 and 4.4 , are selected. The details of the heating condition are presented in **Table 1.** As seen from the table, the heat input rate becomes twice and the speed of the heat source becomes half when the size of the plate becomes two times.

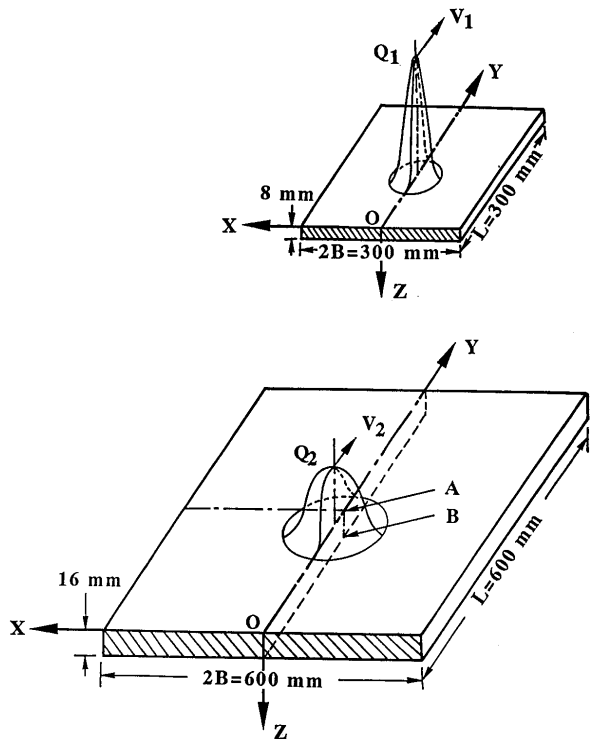

Fig.13 Geometrically similar models.

Table 1 Heating conditions for similarity.

model	ζ	h (mm)	Q (cal/sec)	v (mm/sec)	κ (mm⁻²)
M 8	1.9	8	1107	10	3.1 × 10⁻³
	4.4	8	2475	50	3.1 × 10⁻³
M 1 6	1.9	16	2214	5	7.75× 10⁻⁴
	4.4	16	4950	25	7.75× 10⁻⁴

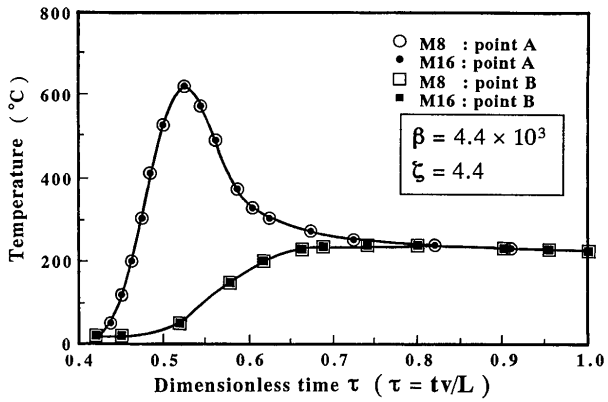

Fig.14 Temperature history at point A and B on top and bottom at mid-length of plate for models M8 and M16 (ζ=4.4).

The time histories of the temperature on the top and the bottom surfaces at the center of the two geometrically similar models are shown in **Figs.14** and **15.** The abscissa represents the dimension less time τ. Though the thickens of the plate h should be used in normalizing the time according to the similarity rule, the length of the plate L is used for convenience. Then, when the normalized time τ is equal to 0.5, the heat source is passing the center of the plate. The open and the solid symbols represent the temperatures of the models **M8** and **M16**, respectively. It is seen from these figures that the temperatures are the same and the similarity holds when β and ζ are the same.

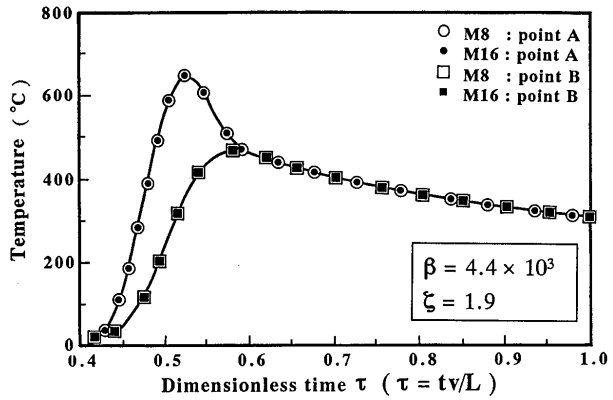

Fig.15 Temperature history at point A and B on top and bottom at mid-length of plate for models M8 and M16 (ζ=1.9).

Further, using temperature fields computed in the above, the thermal-elastic-plastic deformation of the plates are analyzed by F.E.M. The computed results are shown in **Figs.16-18.** Figure 16 shows the time histories of the angular distortion at the starting side of the edge (hatched section in Fig.13). The angular distortions of geometrically similar plates are the same and similarity holds when when β and ζ are the same. It is also seen from the figure that the plate deforms into the convex shape viewed from the heating side in the very first stage. Then the deformation is reversed and the shape becomes concave. If the cases with different ζ are compared, the surface temperatures are roughly the same when β is the same. But the angular distortion is large when ζ or the moving speed is small. The reason for this is that the heat input per unit length is smaller if ζ is large.

Figure 17 shows the transverse shrinkage at the center section of the plate normalized by the half width of the plate B. The similarity can be observed from this figure and it is seen that the magnitude of the shrinkage decreases when ζ becomes large. The same trend can be seen from Fig.18 which shows the distribution of the plastic strain component in the width direction. The

distribution is shown through the thickness at the center of the plate. It is seen that the plastic strain distributes only near the surface when ζ is large. This explains the results that both the angular distortion and the shrinkage become small when ζ is large.

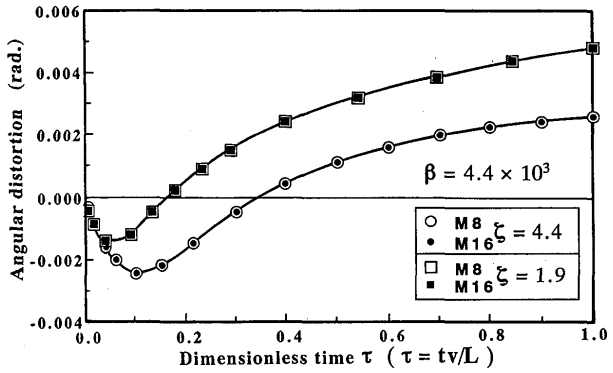

Fig.16 Time history of angular distortion at starting edge for models M8 and M16.

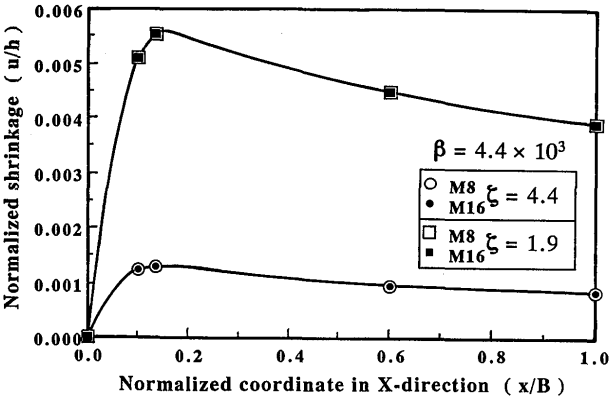

Fig.17 Distribution of shrinkage in transverse direction at mid-length of plate.

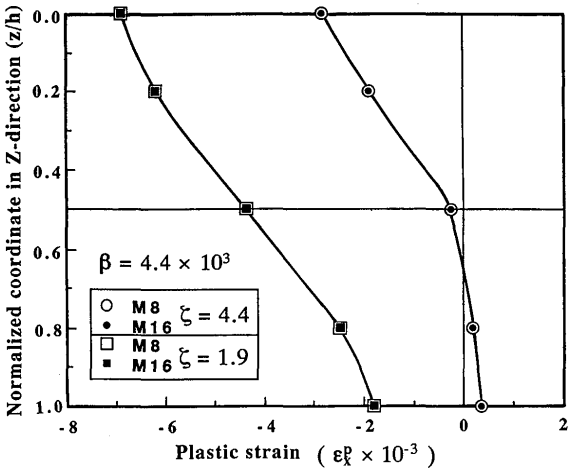

Fig.18 Distribution of plastic strain in X-direction at mid-length through thickness of plate.

5. Heating Conditions and Inherent Deformations

5.1 Models for serial computations

As it is discussed in the previous report[1),2)], the selective use of both the angular distortion and the shrinkage is necessary to achieve an efficient plate bending procedure. For this purpose, appropriate heating conditions to obtain the required angular distortions or shrinkage must be known. At the same time, the comprehensive understanding on the relation between the heating condition and the resulting inherent deformations is necessary to develop new and ideal heating devices.

Since the properties of the heat source can be characterized by the parameters β and ζ, the inherent deformations obtained by the line-heating can be classified using these parameters. The same model as M8 discussed in section 4.3 is used for the parametric study. The distribution of the heat input is assumed also as Gaussian distribution with $\kappa=3.1\times10^{-3}$ mm^{-2}. The ranges of the parameters to be examined are selected according to the practical situation. Since the maximum value of the surface temperature is limited, three values of β are selected, namely $\beta=3.2\times10^3$ ($T_{s,max}$=445°C), $\beta=4.4\times10^3$ ($T_{s,max}$=615°C) and $\beta=5.7\times10^3$ ($T_{s,max}$=785°C). As for ζ, the range which includes the point gives the maximum angular distortion is selected, such that, $0.6 < \zeta < 6.2$.

5.2 Relation between parameters and deformations

The relation between the parameters β, ζ and the computed angular distortion is shown by **Fig.19**. As observed in the figure, the angular distortion increases with β or the surface temperature. From the variation with ζ, it is seen that the angular distortion gives maximum at certain value of ζ when β is constant. The dashed line in the figure is the line connecting the points with the same value of the heat input per unit length Q/v. These lines show that the magnitude of the angular distortion is not determined by Q/v alone. It also depends on how fast the heat is applied.

Similarly, the relation between the parameters and the transverse shrinkage at the center of the plate is shown in **Fig.20**. The shrinkage also increases with β. Though, it is small when the moving speed is large, it rapidly increases as the speed becomes fairly small. **Figure 21** shows the relation between the parameters and the inplane and the bending plastic strains at the center of the plate. The inplane plastic strain component in the transverse direction ε_X^m is represented

by the plastic strain at the midsurface of the plate. The bending component $\varepsilon_x{}^b$ is represented by the difference between the plastic strains at the top and the middle surfaces. Both the inplane and the bending plastic strains in Fig.21 show the same trend as Figs.19 and 20. From these figures, it can be seen that the inplane or the bending dominant deformation can be achieved by selecting proper heating conditions. The bending dominant deformation is obtained when the surface temperature is high and the moving speed of the heat source is fast. The dominant inplane shrinkage deformation is obtained when the moving speed is slow, such that $\zeta < 3.0$.

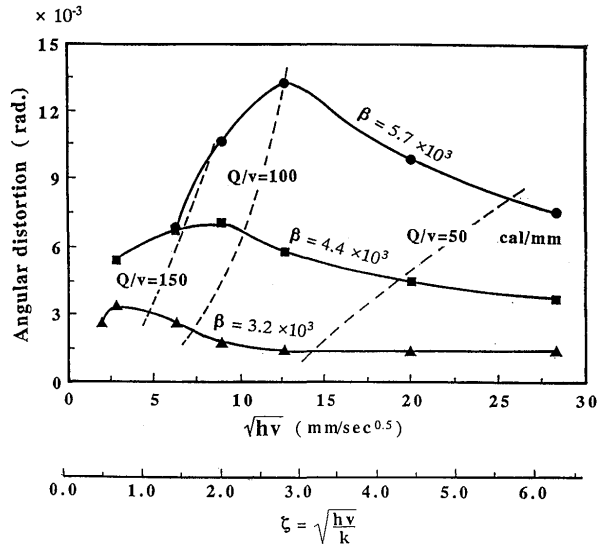

Fig.19 Relation between angular distortion and parameters ζ and β.

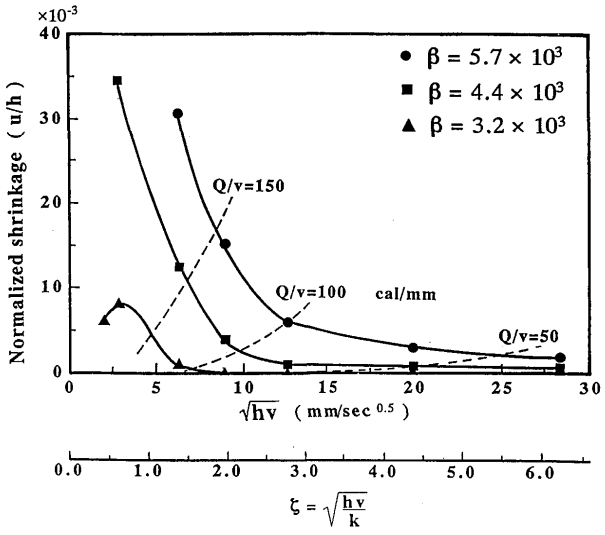

Fig.20 Relation between shrinkage and parameters ζ and β.

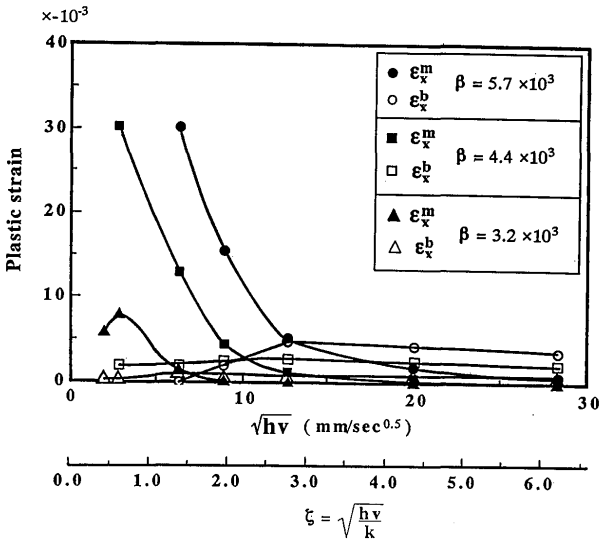

Fig.21 Influence of parameters ζ and β on bending and inplane plastic strains at mid-length of plate.

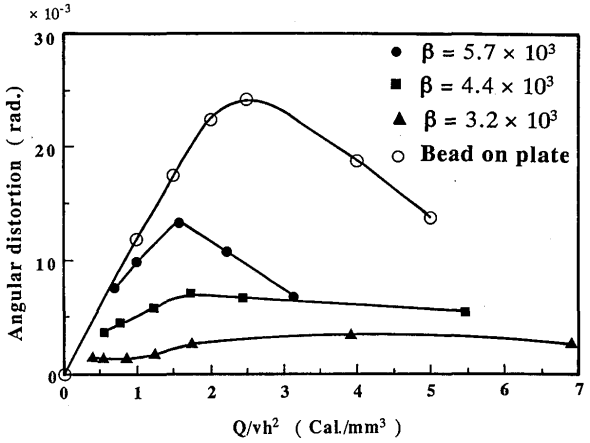

Fig.22 Angular distortion in line heating and welding processes.

The welding is a similar process as the line-heating. The deformation under the welding was studied by Satoh et al.[17] It is shown that the angular distortion by welding is basically governed by one parameter which represents the heat input per unit length divided by the square of the plate thickness (Q/vh^2). For comparison, the angular distortion by the line-heating is plotted against (Q/vh^2) together with those by the welding in **Fig.22**. The significant difference between the welding and the line-heating is the maximum temperature. Since the temperature is much higher in the welding compared to the line-heating, the curve representing the welding locates above those for the line-heating. It is also seen that the lines for line-heating tend to approach to that for the welding when the surface temperature is high (or β is

large) and heat input is small (or the moving speed is fast).

5.3 Effect of heat input distribution

The effect of the primary factors has been discussed in the previous sections. Other factors which may influence the resulting deformation are the heat input distribution, method of cooling, mechanical properties of the plate, the initial curvature and the residual stress. Among these, the heat input distribution is selected and its effect is examined.

The model considered is the same as that shown in section 5.2. The primary parameters are kept same (β=4.4×10^3, ζ=2.8) and three different values of concentration coefficient are considered, namely κ=2.0×10^{-3}, 3.1×10^{-3}, 3.9×10^{-3} mm^{-2}. The computed angular distortion and the shrinkage are compared in **Fig.23.** $T_{s,max}$ in the figure shows the maximum surface temperature for each case. The surface temperature increases as the concentration coefficient becomes large. Due to the temperature increase, both angular distortion and the shrinkage increase. Therefore, it is seen that the heat input distribution is an influential factor on the deformation and it must be controlled as carefully as the primary factors.

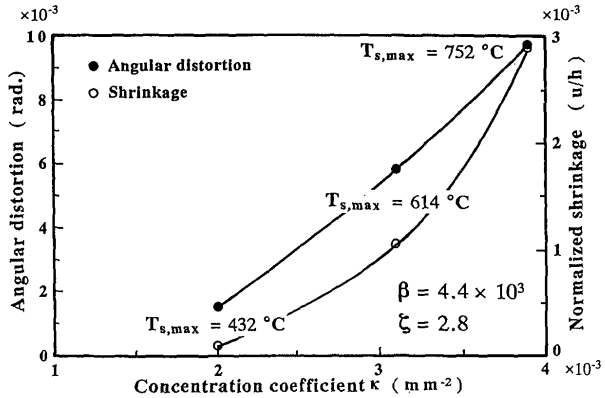

Fig.23 Influence of concentration coefficient of heat input on deformations under line-heating.

6. Conclusions

In order to achieve rational and effective plate bending through the line-heating, it is necessary to know the proper heating conditions to get the inherent deformation required for each heating line. To obtain a general understanding of the phenomenon, the similarity rule governing the line-heating process is studied and two parameters which characterize the heating condition are proposed. The validity of these parameters in the similarity has been examined. For the quantitative study of the plate bending process, a 3-D F.E.M. code for the thermal-elastic-plastic large deformation problem and that for the heat conduction problem are developed. The validity of the developed F.E.M. codes are examined through the comparison with an experiment using the induction heating. Further, the relation between the heating conditions and the inherent deformations has been studied based on the proposed parameters. Through the present study, the following conclusions are drawn.

(1) The plate bending process by the induction heating is analyzed using the F.E.M.code developed in the present research and their validity is proved through the comparison with the experiment.

(2) The proposed conditions for the similarity in line heating process are proved to be correct through numerical simulations.

(3) The relation between the parameters β and ζ, which characterize the heating conditions and the resulting inherent deformations are studied. Through this study, it is shown that the line-heatings specially aiming at the bending or the shrinkage can be achieved by choosing proper heating conditions. To get the angular distortion, β or the surface temperature must be high and the moving speed of the heat source should be fast. On the other hand, to get the shrinkage, ζ or the moving speed must be small enough.

(4) When the welding and the line-heating process are compared, they are the phenomena which have the same nature at the root. The welding is considered as the extreme case of the line-heating when the surface temperature is high and the moving speed is fast. In other word, both β and ζ are large in the welding.

(5) Although the parameters β and ζ are kept same, the deformation changes with the distribution of the heat input. It is shown that both the angular distortion and the shrinkage become large when the heat input is concentrated.

References

1) Y. Ueda, H. Murakawa, A. M. Rashwan, Y. Okumoto, R. Kamichika, "Development of Computer Aided Process Planning System for Plate Bending by Line-Heating, (1st Report) Relation between the Final Form of the Plate and the Inherent Strain", Journal of The Society of Naval Architects of Japan, Vol. 170 (1991), pp. 577-586 (in Japanese).

2) Y. Ueda, H. Murakawa, A. M. Rashwan, Y. Okumoto, R. Kamichika, "Development of Computer Aided Process Planning System for Plate Bending by Line-Heating, (2nd Report) Practice for Plate Bending in Shipyard Viewed from Aspect of Inherent Strain",

Journal of The Society of Naval Architects of Japan, Vol. 171 (1992), pp. 83-93 (in Japanese).
3) I. Tsuji, "Studies of Longitudinal Distortion of Mild Steel Plate in Gas Cutting Operation", Journal of the Japan Welding Society, Vol. 26, No.2 (1957), pp.96-102 (in Japanese).
4) T. Suhara, "Study of Thermo Plastic Working: Bending of Beam of Rectangular Cross Section, "Journal of Zosen Kyokai, Vol.103, 1958, pp.233-243 (in Japanese).
5) K. Satoh, S. Matsui, K. Terai and Y. Iwamura, "Water-cooling Effect on Angular Distortion Caused by the Process of Line Heating in Steel Plates", Journal of The Society of Naval Architects of Japan, Vol. 126 (1969), pp. 445-458 (in Japanese).
6) M. Araki, N. Inoue, M. Horioka and M. Ando, "On Angular Distortion of Hull Steel Plates by Line Heating Methods", Journal of The Society of Naval Architects of Japan, Vol.133 (1973), pp. 343-348 (in Japanese).
7) Y. Iwasaki, Hirabe, R. Taura, A. Hujikura and H. Shiota, "Study on the Forming of Hull Plate by Line Heating," Mitusbihsi Juko Giho, Vol.12, No.3, (1975-5), pp. 51-59 (in Japanese).
8) Y. Iwamura. and E. F. Rybicki, "A Transient Elastic-Plastic Thermal Stress Analysis of Flame Forming", Transactions of ASME, Journal of Engineering for Industry, February 1973, pp. 163-171.
9) I. Tsuji and K. Ogawa, "An Analysis on Transient Stress and Deformation of a Steel Strip Subjected to Local Heating", Journal of the Japan Welding Society, Vol.45, No.1 (1976), pp.36-41 (in Japanese).
10) A. Moshaiov and W. S. Vorus, "The Mechanics of the Flame Bending Process: Theory and Applications", Journal of Ship Research, Vol.31, No. 4 (Dec. 1987), pp. 269-281.
11) A. Moshaiov and J. G. Shin, "Modified Strip Model for Analyzing the Line Heating Method (Part 2): Thermo-Elastic-Plastic Plates", Journal of Ship Research, Vol.35, No.3 (Sept. 1991), pp. 266-275.
12) T. Nomoto, T. Ohmori, T. Sutoh, M. Enosawa, K. Aoyama and M. Saitoh, "Development of Simulator for Plate Bending by Line-Heating", Journal of The Society of Naval Architects of Japan, Vol.168 (1990), pp.527-535 (in Japanese).
13) Y. Ueda and T. Yamakawa, "Analysis of Thermal Elastic-Plastic Stress and Strain during Welding by Finite Element Method", Journal of the Japan Welding Society, Vol.2, No.2 (1971), pp.90-100.
14) T. J. R. Hughes, R. L. Taylor and W. Kanoknukulchai, "A Simple and Effective Finite Element Element for Plate Bending", International Journal of Numerical Methods in Engineering, Vol.11 (1977), pp.1529-1543.
15) Y. Ueda, H. Murakawa and H. Masuda, "Locking Phenomena in Elastic-Plastic Buckling Analysis by Finite Element Method", Proc. 9th Symposium on Numerical Analysis of Structures, Tokyo (1985), pp.311-316.
16) K. Scully "Laser Line Heating", Journal of Ship Production, Vol.3, No. 4 (1987), pp. 237-246.
17) K. Satoh and T. Terasaki, "Effect of Welding Conditions on Welding Deformations in Welded Structural Materials", Journal of the Japan Welding Society, Vol.45 ,No.4 (1976), pp.302-308.
18) D. I. H. Barr, "A Survey of Procedures for Dimensional Analysis", Int. J. Mech. Eng. Educt., Vol. 11, No.3 (1982), pp. 147-159.
19) O. Aono, "Dimensions and Dimensional Analysis", Kyoritsu-Shuppan, (1982), (in Japanese).
20) W. M. Rohsenow J. P. Hartnett, "Handbook of Heat Transfer", Section 3: Conduction, McGraw-Hill, Inc., (1973).
21) U. Grigull and H. Sandner : Heat Conduction, Springer-Verlag, (1984).

Appendix

Similarity Rule

As a method to derive conditions or parameters for the similarity, dimensional analysis[18),19)] is commonly used. Also parameters can be derived as the coefficients of governing equations and boundary conditions in dimensionless form. On the other hand, the line-heating process can be divided into the thermal conduction analysis and the thermal-elastic-plastic analysis. The dimensional analysis is employed for the heat conduction problem and the method based on the dimensionless equations is applied for the deformation problem.

1. Deformation problem

When the transient temperature field is known, the deformation problem is described by the compatibility equations, the constitutive equations, the equilibrium equations and the boundary conditions in the incremental form. To normalize the variables, the plate thickness h and the yield stress σ_{Y0} are selected as fundamental quantities. The governing equations and the boundary conditions are transformed into the following dimensionless form using h and σ_{Y0}.

(a) compatibility condition

$$\hat{\varepsilon}_{ij} = \frac{1}{2}\left(\hat{u}_{i,j} + \hat{u}_{j,i} + \hat{u}_{k,i}\,\hat{u}_{k,j}\right) \quad \text{(a.1)}$$

where,

$$\hat{u}_{i,j} = \partial \hat{u}_i / \partial \hat{x}_j$$
$$\hat{x}_j = x_j/h \ , \quad \hat{u}_i = u_i/h$$

(b) constitutive relation (elastic-perfect-plastic)

The constitutive relation for the elastic-perfect-plastic material is described by the following set of equations.

· separation of strain increment

$$\Delta\hat{\varepsilon}_{ij} = \Delta\hat{\varepsilon}^{e}_{ij} + \Delta\hat{\varepsilon}^{p}_{ij} + \Delta\hat{\varepsilon}^{T}_{ij} \quad \text{(a.2)}$$

where, $\Delta\hat{\varepsilon}^{e}_{ij}$, $\Delta\hat{\varepsilon}^{p}_{ij}$, $\Delta\hat{\varepsilon}^{T}_{ij}$ denote the elastic, the plastic and the thermal strain increments. Using the thermal expansion ratio α and the temperature increment ΔT, the thermal strain increment $\Delta\hat{\varepsilon}^{T}_{ij}$ is defined as,

$$\Delta\hat{\varepsilon}^{T}_{ij} = \underline{\alpha\,\Delta T}\,\delta_{ij} \quad \text{(a.3)}$$

· strain increment

$$\Delta\hat{\sigma}_{ij} = \underline{(2\mu/\sigma_{Y0})}\,\Delta\hat{\varepsilon}^{e}_{ij} + \underline{(\lambda/\sigma_{Y0})}\,(\Delta\hat{\varepsilon}^{e}_{mn}\delta_{mn})\,\delta_{ij} + \underline{2\,(\partial\mu/\partial T)\,(\Delta T/\sigma_{Y0})}\,\hat{\varepsilon}^{e}_{ij} \quad \text{(a.4)}$$

$+\underline{(\partial\lambda/\partial T)\ (\Delta T/\sigma_{Y0})}\ (\hat{\varepsilon}^{e}_{mn}\delta_{mn})\ \delta_{ij}$

where, μ and λ are Lame's coefficients.

· yield condition

$$(3/2)\ \hat{s}_{ij}\Delta\hat{s}_{ij} = \underline{2\ (\sigma_Y/\sigma_{Y0})(\partial\sigma_Y/\partial T)(\Delta T/\sigma_{Y0})} \quad (a.5)$$

where, $\hat{s}_{ij}$ is the normalized deviatoric stress component which is defined as,

$$\hat{s}_{ij} = \{\sigma_{ij} - \tfrac{1}{3}(\sigma_{mn}\delta_{mn})\ \delta_{ij}\}/\sigma_{Y0} \quad (a.6)$$

· normality rule

$$\Delta\hat{\varepsilon}^{p}_{ij}\Delta\hat{s}_{ij} = 0 \quad (a.7)$$

(c) equilibrium equation (no body force acting)

$$\partial\hat{\sigma}_{ij}/\partial\hat{x}_j = 0 \quad (a.8)$$

(d) boundary conditions (no external force acting)

$$n_j\ \hat{\sigma}_{ij} = 0 \quad (a.9)$$

where n_j is the component of the outward normal to the surface of the body. The similarity holds when the coefficients which are indicated by underlines are the same. Therefore, if the material properties μ, λ, σ_{Y0} and α are the same including their dependence on temperature, the similarity holds for the geometrically similar models when the temperature T is the same.

2. Heat conduction problem

The temperature field in the line-heating process is mainly governed by the heat conductivity λ, the heat capacity per unit volume C_p, the thickness of the plate h, the heat input rate Q, the moving speed of heat source v and the maximum surface temperature under heating T_{max}. Denoting the dimensions of length, force, time and temperature as L, F, t and T, respectively, the above values have the following dimensions.

$$\begin{aligned}
[\lambda] &= [L^0, F^1, t^{-1}, \theta^{-1}] \quad (a.10)\\
[C_p] &= [L^{-2}, F^1, t^0, \theta^{-1}]\\
[h] &= [L^1, F^0, t^0, \theta^0]\\
[Q] &= [L^1, F^1, t^{-1}, \theta^0]\\
[v] &= [L^1, F^0, t^{-1}, \theta^0]\\
[T_{max}] &= [L^0, F^0, t^0, \theta^1]
\end{aligned}$$

According to Rayleigh's method[18], the temperature T can be expressed as,

$$T = G(\lambda^a, C_p^b, h^c, Q^d, v^e, T_{max}^f) \quad (a.11)$$

Further, the dimensional relation of the above equation is shown to be,

$$\theta = (F\ t^{-1}\theta^{-1})^a (L^{-2}\ F\theta^{-1})^b (L)^c (L^1\ F\ t^{-1})^d \times (L\ t^{-1})^e\ (\theta)^f \quad (a.12)$$

Since, the dimensions of the both sides of Eq.(a.12) must be the same, the following relations are derived.

$$\begin{aligned}
1 &= -a - b + f\\
0 &= a + b + d\\
0 &= -2b + c + d + e\\
0 &= -a - d - e
\end{aligned} \quad (a.13)$$

By eliminating b, c, e, f from the above four equations, the normalized temperature T/T_{max} can be written as,

$$T/T_{max} = \Psi\ (\{\lambda/C_p vh\}^a \{Q/C_p h^2 v T_{max}\}^d) \quad (a.14)$$

Noting that a and d are arbitrary, the terms in the two sets of parentheses must be the same for the similarity to hold, such that,

$$\begin{aligned}
c_1 &= \lambda/C_p vh \quad (a.15)\\
c_2 &= Q/C_p h^2 v T_{max}
\end{aligned}$$

As it is discussed, the temperature must be the same for the similarity in the deformation problem. Thus, the maximum surface temperatures in mutually similar models are the same. Under such condition, Eq.(a.15) can be rewritten as,

$$\begin{aligned}
c_1 &= \lambda/C_p vh \quad (a.16)\\
c_3 &= Q/C_p h^2 v
\end{aligned}$$

Further, the condition that "both c_1 and c_2 are the same" and the condition that "two independent combinations of these are the same" are identical. Thus, the following two parameters which govern the similarity are derived.

$$\begin{aligned}
\zeta &= (c_1)^{-1/2} = (vh/k)^{1/2} \quad (a.17)\\
\beta &= (c_1)^{-1/2} c_3 = Q/p(vh^3)^{1/2}
\end{aligned}$$

where,

k: thermal diffusivity

$$k = \lambda/C_p$$

p: coefficient of heat penetration

$$p = (\lambda C_p)^{1/2}$$

Physically, the parameter ζ corresponds to the similarity condition for the general quasi-steady heat conduction problem under heat source moving at constant velocity. It is the same as the coefficient of the governing equation in dimensionless form, such that,

$$\nabla^2\hat{T} = \underline{(vh/k)}\ (\partial\hat{T}/\partial\hat{x}) \quad (a.18)$$

On the other hand, the parameter β has the dimension of temperature and its value corresponds to the maximum surface temperature.

In the above discussion, the parameters defined by Eq.(a.15) are dimensionless values. It is natural to adopt dimensionless values to describe conditions for similarity. However, since the parameter is defined only by Q, v, h and material constants and it is related to the maximum surface temperature, the parameter β defined by Eq.(a.17) is adopted in this report.